

## **Noise-Resilient Statistical Framework for Multi-Region Satellite Image Classification Using Run-Length and Gradient-Based Descriptors and a Hybrid Statistical Approach**

**Reem tallal Kamil**

[Reem@copew.uobaghdad.edu.iq](mailto:Reem@copew.uobaghdad.edu.iq)

### **Abstract**

Gaussian noise represents a significant challenge in satellite image processing, as it distorts pixel level relationships and compromises the fidelity of spatial data. This degradation hinders accurate land-cover classification, which is essential for applications such as urban planning, environmental monitoring, and resource management. To address this issue, this study proposes an enhanced hybrid statistical framework designed to classify satellite images into three primary regions (urban, vegetation, and water) even under significant noise interference. The core innovation of this research lies in a dual-stage processing pipeline that integrates texture and structural feature extraction with proactive noise suppression. First, a median filter is applied to mitigate Gaussian noise while preserving critical edge information. Subsequently, two complementary feature descriptors are employed: the Gray-Level Run-Length Matrix (GLRLM), which captures texture patterns through the analysis of consecutive pixel runs, and the Histogram of Oriented Gradients (HOG), which encodes local shape and edge information through gradient orientation distributions. The fusion of these features provides a robust and discriminative representation of land-cover types. The proposed framework was rigorously evaluated using Sentinel-2 imagery of Shanghai, subjected to varying levels of synthetic Gaussian noise (0%, 5%, 10%, and 20%). Performance was assessed using multiple quantitative metrics: Mean Squared Error (MSE), Peak Signal-to-Noise Ratio (PSNR), Structural Similarity Index (SSIM), Classification Accuracy (ACC), and Execution Time. Experimental results demonstrate the superiority of the hybrid approach. At 20% noise, the proposed method achieved an exceptional classification accuracy of 98.55%, alongside a PSNR of 122.45 dB and an SSIM of 0.98. In contrast, conventional GLRLM and HOG methods exhibited

significant performance degradation under noise, with accuracies fluctuating widely and structural integrity compromised. The hybrid framework also produced a more realistic and balanced distribution of land-cover areas, correctly identifying urban regions that were often misclassified by traditional methods.

**Keyword:**

Satellite Image Classification, Gaussian Noise Reduction, Median Filtering, Gray-Level Run Length Matrix (GLRLM), Histogram of Oriented Gradients (HOG), Hybrid Statistical Approach, Remote Sensing, Image Restoration, Feature Fusion.

**1. Introduction:**

Satellite imagery is crucial for modern remote sensing, significantly enhancing our understanding of Earth's surface and environmental changes. It offers detailed insights into natural resources and urban development, making it essential for researchers and decision-makers. The effectiveness of this imagery, however, relies on high-quality data free from technical defects [16]. The process of capturing images via spaceborne sensors introduces "image noise" or distortion, which affects the quality and accuracy of topographic analyses. This noise leads to the loss of fine details, making it crucial to obtain noise-free images to ensure valid results in image processing. Inaccurate studies resulting from distorted images can lead to poor planning decisions or flawed environmental assessments [2]. Gaussian noise is a prevalent and challenging distortion in digital image processing, often caused by sensor circuit disturbances or unfavorable lighting and thermal conditions. Its statistical distribution affects all grayscale levels, complicating the differentiation between actual pixels and noise. Therefore, immediate denoising is crucial; failing to address this before analysis can undermine the reliability of feature extraction [20].

In this context, the fundamental role of statistical methods emerges as a bridge connecting advanced statistics with digital image processing. The link between these two fields represents a modern and effective trend; an image is, in reality, nothing more than a matrix of digital data subject to the laws of probability distributions and statistical variances. Statistical methods allow researchers to analyze spatial patterns and interrelationships between adjacent pixels, contributing to a deeper understanding of the image's texture. Toward robust satellite image classification, "image classification" stands out as one of the most important fruits of this statistical-image link. Classification aims to categorize the image into specific thematic classes based on its digital characteristics. The benefits of

classification are evident in its ability to transform raw data into informational maps showing the distribution of urban, agricultural, and water areas with high accuracy, facilitating spatial inventory operations and land-use monitoring.

This paper relies on robust statistical methods that have proven efficient in analyzing image textures, namely the Gray-Level Run Length Matrix (GLRLM) and Histogram of Oriented Gradients (HOG). The justification for choosing these methods lies in their high ability to describe spatial relationships between pixels—crucial features in satellite images where terrains overlap complexly. However, given the challenges posed by Gaussian noise, which may weaken the performance of these traditional methods, a "Hybrid Method" is proposed in this study. The rationale for proposing this hybrid approach stems from the need to integrate proactive noise processing capabilities with precise statistical feature extraction, aiming to achieve a "robust" classification that remains unaffected by fluctuations in noise levels. This ensures the maintenance of classification accuracy between urban, agricultural, and water regions even under the harshest imaging conditions.

Based on a number of basic statistical measures of image quality, a comparison will be made between the statistical methods used to select the best method for achieving the purpose of this paper. The data used are the color gradient levels of the image pixels that make up an image taken of Shanghai City, China.

## **2. Literature Review:**

Many researchers and specialists in this field have sought to study the problem of noise and its impact on the accuracy of spatial data using the aforementioned statistical methods, attempting to find solutions that balance execution speed with result accuracy. From this standpoint, we will address a review of the most important previous studies that laid the initial foundations in this paper path and contributed to the development of the tools we use today.

Lee et al. (2010) [14] presents a human detection system combining motion extraction, human body ratio estimation, and Histogram of Oriented Gradients (HOG) features. Tested across various environments, the system achieved up to 95% detection rate in controlled settings but performed poorly under occlusion and noise. The authors suggest integrating gamma correction and Local Binary Patterns to improve robustness in future work. Kelly et al. (2014) [12] proposes an FPGA-based multi-core processor (IPPro) for real-time HOG feature extraction in pedestrian detection. The design optimizes memory access and

computational efficiency, achieving high throughput (209 fps) with lower power consumption compared to GPU and hand-coded FPGA solutions. The approach offers scalability, programmability, and reduced development time, making it suitable for embedded vision applications. Mehta & Aggarwal. (2014) [15] focused on optimizing Median filters for high-density noise removal. The researchers developed adaptive filtering techniques that balance the trade-off between noise suppression and detail preservation, proving that refined Median-based approaches are essential for modern high-resolution image processing. Da Costa et al. (2016) [4] focused on the segmentation of satellite images by comparing various techniques. The authors highlighted the critical role of preprocessing in satellite data, noting that noise interference often complicates the classification of different land cover types, which necessitates the use of robust feature extraction methods. Kairuddin & Mahmud (2017) [10] investigates texture feature extraction from kidney ultrasound images across different machine resolutions. Using Gaussian filtering for denoising and statistical methods (IH, GLCM, GLRLM), the authors identified three GLCM features—Contrast, Difference Variance, and Inverse Difference Moment Normalized—that remain statistically invariant regardless of image quality, suggesting their reliability for characterizing healthy kidney tissue in computer-aided diagnosis systems. Novitasari et al. (2019) [17], investigated texture analysis methods for classifying mammogram images into normal, benign, and malignant categories. They compared four statistical feature extraction techniques: First-Order Statistics, Gray Level Co-occurrence Matrix (GLCM), Gray Level Run Length Matrix (GLRLM), and Gray Level Difference Method (GLDM). The extracted features were classified using an Error-Correcting Output Codes Support Vector Machine (ECOC-SVM) with linear, RBF, and polynomial kernels. Their results indicated that the GLRLM method combined with a polynomial kernel SVM yielded the best performance, achieving an accuracy of 93.98%, highlighting GLRLM's effectiveness in capturing discriminative textural patterns for breast cancer diagnosis. Zhang et al. (2019) [26], addressed the computational bottleneck in extracting Gray Level Run Length Matrix (GLRLM) texture features from high-resolution medical images like MRIs. Recognizing that GLRLM construction is tedious for many regions of interest (ROIs), they proposed a novel GPU-accelerated paradigm using parallel primitives (via CUDA and the CUB library). Their method simultaneously processes multiple overlapping ROIs within a single image. Experiments demonstrated a significant speedup of over 5x compared to an optimized serial implementation, offering a practical solution for real-time or large-scale medical image analysis where texture-based features are crucial for tasks like lesion

detection and classification. Vara et al. (2020) [24] examines how Time Gain Compensation (TGC) settings in ultrasound imaging affect texture analysis metrics. Through analysis of liver and kidney images using first- and second-order features, the study finds that most texture indices are significantly influenced by TGC, with optimal analysis occurring around 50% TGC. The work highlights the need to standardize TGC in radiomic studies to ensure reproducibility and avoid feature variability. Ding et al. (2021) [7] investigated the impact of Gaussian noise on image quality and explored various denoising strategies. The researchers emphasized that Gaussian noise, often originating during image acquisition, significantly degrades visual information, and they advocated for advanced filtering techniques to restore image clarity for subsequent analysis. Ochango et al. (2022) [18], explored feature extraction methods for classifying maize leaf diseases (common rust, leaf spot, northern leaf blight) from healthy leaves. They compared three descriptors: ORB, KAZE, and HOG. Following feature extraction, multiple machine learning classifiers were evaluated. Their experimental results showed that HOG features consistently outperformed ORB and KAZE when used with various classifiers. The Random Forest algorithm achieved the best classification results using HOG features, with an accuracy of 74%, precision of 77%, recall of 77%, and an F1-score of 75%. This study validated HOG's robustness for agricultural image-based disease diagnosis. Ashraf et al. (2024) [3] conducted an evaluation of different noise reduction filters, specifically comparing Median filters with other spatial filters. The study concluded that Median filtering is particularly effective in removing impulse noise while preserving the sharp edges of objects within the image, which is vital for maintaining the structural integrity of satellite data. Kayathri & Kavitha (2024) [11], proposed an integrated "CGSX Ensemble" framework for diabetic retinopathy (DR) severity classification. The approach combines deep learning (CNN for automatic feature extraction), Grey Wolf Optimizer (GWO for feature selection), and ensemble classifiers (SVM and XGBoost). The model was evaluated on retinal fundus images, employing pre-processing techniques like CLAHE and Anisotropic Diffusion Filtering. Their proposed ensemble significantly outperformed standalone ML and DL models, achieving a top accuracy of 93%, along with 94% precision, 93% recall, and a 94% F1-score. This represents a substantial improvement over a baseline EfficientNet model (88% accuracy), demonstrating the value of hybrid feature extraction and selection strategies for complex medical image analysis. Sadeeq et al. (2024) [21], proposed a passive method for detecting image forgeries (splicing and copy-move) using the Histogram of Oriented Gradients (HOG) descriptor. The method extracts HOG features from the high-frequency sub-bands

(LH, HL, HH) of the Discrete Wavelet Transform (DWT) applied to images in the YCbCr color space. These features are then fed to a Multilayer Perceptron classifier. Evaluated on the CASIA v1.0 and v2.0 datasets, the method achieved promising accuracies of 91.45% and 89.67%, respectively. The study also found that an 8x8 pixel block size for HOG extraction yielded optimal results and demonstrated superior performance compared to some co-occurrence matrix-based methods.

The progression of these studies illustrates a clear trend from the establishment of basic statistical descriptors (GLRLM and HOG) to the development of sophisticated denoising frameworks. While early research focused on feature extraction, more recent studies underscore the necessity of robust preprocessing, such as Median filtering, to handle the persistent challenge of Gaussian noise. This paper builds upon these foundations by proposing a hybrid system that integrates these established techniques into a unified, noise-resistant classification pipeline.

### **3. Theoretical Part:**

This section provides the theoretical foundation for the research, bridging the gap between digital image fundamentals and the advanced statistical methods used for classification.

#### **3.1 Digital Image Fundamentals:**

A digital image is a discrete representation of a physical scene, structured as a two-dimensional matrix of numerical values called pixels (picture elements). Each pixel represents the intensity of light or energy captured at a specific spatial coordinate (x, y). For a grayscale image, the intensity  $f(x,y)$  typically ranges from 0 (black) to 255 (white) in an 8-bit system [27]. Digital images are characterized by spatial resolution (detail level) and radiometric resolution (intensity depth). The mechanism involves sampling (spatial discretization) and quantization (converting continuous light levels into integer values), forming the basis for any mathematical or statistical analysis.

#### **3.2 Satellite Imagery:**

Satellite images are a specialized form of digital data captured by spaceborne sensors (multispectral or panchromatic). These images provide a macroscopic view of the Earth, capturing data beyond the visible spectrum (such as Infrared or Thermal). They are vital in Environmental Monitoring (tracking deforestation), Urban Planning (managing city growth), Agriculture (yield prediction), and Disaster Management (flood and wildfire

assessment). Their ability to cover vast, inaccessible areas makes them indispensable for global geographic information systems (GIS) [6].

### 3.3 Image Noise:

Noise is the undesirable alteration of pixel values that masks the true information in an image. In satellite sensors, noise is primarily caused by electronic interference, thermal agitation in circuits (Gaussian Noise), or transmission errors during data uplink/downlink. Gaussian Noise, characterized by a probability density function (PDF) equal to the normal distribution [9]:

$$P(z) = \frac{1}{\sqrt{2\pi\sigma^2}} e^{-\frac{(z-\mu)^2}{2\sigma^2}} \quad (1)$$

Where: (z) Gray level, ( $\mu$ ) average intensity of noise, ( $\sigma$ ) intensity of noise fluctuation. Noise degrades structural details and creates "false textures," leading to classification errors. Denoising is the process of recovering the original signal to ensure that the statistical analysis reflects the actual terrain rather than sensor artifacts.

### 3.4 Statistical Classification Methods:

#### A. Gray-Level Run Length Matrix (GLRLM):

The GLRLM is a statistical method for extracting texture features from grayscale images, based on analyzing consecutive pixel sequences (runs) with the same intensity level. First developed in the 1970s, it has wide applications in image classification, particularly in medical fields (radiology, histopathology) and remote sensing [5]. The working mechanism of this method can summarize in: Gray-level quantization which Reduce intensity levels (e.g., from 256 to 8-16 levels). Run detection, for each angle  $\theta$ , scan the image to identify consecutive runs. And matrix population, for each run with length  $j$  and intensity level  $i$ , increment  $P(i, j)$  by one. Gray-Level Run Length Matrix (GLRLM) is a second-order statistical method that characterizes texture by measuring the length of consecutive pixels (runs) having the same gray-level value in a given direction. Unlike GLCM, which considers only pairwise pixel relationships, GLRLM captures extended spatial dependencies, making it less sensitive to pixel-level noise fluctuations [22]. The run is defined as a sequence of adjacent pixels with identical gray levels occurring in a specified direction  $\theta$ . The GLRLM is a matrix  $R(i, j | \theta)$ , and the normalized GLRLM is defined as:

$$\hat{R}(i, j) = \frac{R(i, j)}{\sum_{i=1}^G \sum_{j=1}^R R(i, j)} \quad (2)$$

Where:  $(i)$  represents the gray level,  $i = 1, 2, \dots, G$ .  $(j)$  represents the run length,  $j = 1, 2, \dots, R$ . And  $(R(i, j | \theta))$  denotes the number of runs with gray level  $i$  and length  $j$  in direction  $\theta$ .

### B. Histogram of Oriented Gradients (HOG):

The Histogram of Oriented Gradients (HOG) is a feature descriptor used in computer vision and image processing for object detection, particularly human detection. It was introduced by Navneet Dalal and Bill Triggs in 2005 and has become fundamental in many computer vision applications. HOG captures the distribution of gradient orientations in localized portions of an image, essentially describing the shape and appearance of objects through their edge information [13]. HOG is a structural descriptor that captures the distribution of local intensity gradients and edge directions within an image. Instead of relying on absolute pixel intensities, HOG focuses on shape and geometric information, which remains relatively stable under Gaussian noise [23]. Given an image  $I(x, y)$ , the horizontal and vertical gradients are computed as:

$$G_x(x, y) = I(x + 1, y) - I(x - 1, y) \quad (3)$$

$$G_y(x, y) = I(x, y + 1) - I(x, y - 1) \quad (4)$$

The gradient magnitude and orientation are then calculated as:

$$M(x, y) = \sqrt{G_x^2(x, y) + G_y^2(x, y)} \quad (5)$$

$$\theta(x, y) = \tan^{-1} \left( \frac{G_y(x, y)}{G_x(x, y)} \right) \quad (6)$$

The image is divided into small spatial regions called *cells*. For each cell, a histogram of gradient orientations is constructed, weighted by the gradient magnitude:

$$H_k = \sum_{(x, y) \in \text{cell}} M(x, y) \cdot \delta(\theta(x, y) \in \text{bin}_k) \quad (7)$$

Where:  $(H_k)$  is the histogram value of the  $k$ -th orientation bin. And  $(\delta(\cdot))$  is an indicator function.

### C. The Proposed Hybrid Method:

The proposed method is a multi-stage statistical pipeline designed for robustness. It acknowledges that traditional GLRLM and HOG fail under high noise. The mechanism of the proposed method summarized in these points:

- Adaptive Pre-processing: Utilizes a non-linear Median Filter to remove impulsive components of Gaussian noise without blurring edges.
- Contrast Enhancement: Applies Histogram Equalization to expand the dynamic range of the statistical features.
- Hybrid Feature Fusion: Combines the global spatial relationships of GLRLM with the local structural patterns of HOG.

By hybridizing these techniques, the system achieves "Noise-Invariant Classification," ensuring that the 3-region maps (Urban, Vegetation, Water) remain accurate even when the signal-to-noise ratio (SNR) is low. The proposed hybrid method represents a statistically grounded framework designed to address two fundamental challenges in satellite image classification, signal degradation due to Gaussian noise and reliable feature extraction under uncertainty. From a statistical perspective, its importance lies in:

- Noise Distribution Management: Gaussian noise follows a normal distribution  $N(\mu, \sigma^2)$  that contaminates pixel values. Traditional methods like GLRLM and HOG directly analyze noisy data, leading to biased parameter estimates. The proposed method first applies median filtering, which acts as a robust estimator of location that minimizes the influence of outliers (noise spikes) while preserving edges, a critical advantage over mean filtering.
- Variance Stabilization: Noise increases the variance within homogeneous regions, blurring class boundaries. By preprocessing with a median filter, we effectively reduce within-class variance ( $\sigma_{within}^2$ ) while maintaining between-class variance ( $\sigma_{between}^2$ ), thereby enhancing the fisher discriminant ratio for subsequent classification.
- Complementary Feature Spaces: GLRLM captures second-order spatial dependencies (run-length statistics), while HOG encodes first-order gradient distributions. Their fusion creates a high-dimensional feature vector that spans both global texture patterns and local edge structures, providing a more statistically complete representation of land cover types.
- Bias-Variance Tradeoff Optimization: Individual descriptors may suffer from high bias (oversimplification) or high variance (noise sensitivity). The hybrid approach balances this

tradeoff by combining multiple weak estimators into a stronger, more stable classifier with reduced generalization error.

- **Multivariate Normal Approximation:** After denoising, pixel intensities within each region approximately follow multivariate normal distributions. The hybrid features provide sufficient statistics to estimate the parameters  $(\mu, \Sigma)$  of these distributions, enabling Bayesian classification with optimal decision boundaries.

Before extracting statistical features, the proposed method employs a non-linear spatial filter known as the Median Filter. This technique is specifically chosen for its superior ability to suppress Gaussian while preserving the sharpness of edges, which is critical for satellite land-cover boundaries. It operates by sliding a window (kernel) over the image, replacing the center pixel's intensity with the median value of all pixels within that window. For a pixel at location  $(x, y)$  and a neighborhood window  $S_{(x,y)}$ .

$$\hat{f}_{(x,y)} = \text{median}\{g(s, t)\} \quad (8)$$

Where:  $(s, t) \in S_{(x,y)}$ ,  $g(s, t)$  the noisy pixel values within the defined neighborhood,  $\hat{f}_{(x,y)}$  the restored (denoised) pixel value,  $S_{(x,y)}$  the sub-image window (e.g.,  $3 \times 3$  or  $5 \times 5$  matrix).

The proposed approach is a sequential hybrid framework. It acknowledges that statistical descriptors like GLRLM and HOG are highly sensitive to pixel-level fluctuations caused by noise. The workflow Logic of the Proposed Hybrid Method (Structural Robustness) as the point:

- **Stage I (Restoration):** Applies the Median Filter to stabilize the pixel distribution and eliminate Gaussian outliers.
- **Stage II (Enhancement):** Uses Histogram Equalization to improve the "separability" between classes (Urban, Vegetation, Water).
- **Stage III (Fusion):** Extracts HOG features for local detail and GLRLM features for global spatial context.
- **Theoretical Advantage:** This hybridization ensures that the classification is based on the "underlying structural geometry" of the terrain rather than the "stochastic interference" of the noise.

For noise model and filtering. Let the observed noisy image be represented as:

$$I_{noisy}(x, y) = I_{true}(x, y) + \eta(x, y) \quad (9)$$

where  $\eta(x, y) \sim N(\mu, \sigma^2)$  is additive white Gaussian noise.

The median filter operation is defined statistically as:

$$I_{noisy}(x, y) = median\{I_{noisy}(s, t) : (s, t) \in W(x, y)\} \quad (10)$$

where  $W(x, y)$  is a window of size  $k \times k$  centered at  $(x, y)$ .

The statistical property of the median estimator is that it minimizes the expected absolute deviation:

$$\hat{\theta}_{median} = argmin_{\theta} E[|I - \theta|] \quad (11)$$

This makes it more robust to heavy-tailed noise distributions than the mean estimator. This statistical foundation demonstrates that the proposed hybrid method is not merely an empirical combination of techniques, but a principled approach grounded in statistical theory, probability distributions, and optimal estimation principles. The mathematical formulations provide a rigorous framework for understanding why the method outperforms individual descriptors, particularly in

### 3.5 Evaluation Metrics:

The following metrics are used to quantitatively evaluate the results:

#### A. Mean Squared Error (MSE):

MSE measures the average squared difference between the original (clean) image and the processed (denoised/classified) image. A lower MSE indicates higher similarity and less distortion [8].

$$MSE = \frac{1}{M \times N} \sum_{i=0}^{M-1} \sum_{j=0}^{N-1} [I(i, j) - K(i, j)]^2 \quad (12)$$

Where: M, N, the dimensions of the image (rows and columns),  $I(i, j)$  the intensity value of the pixel in the original image,  $K(i, j)$  the intensity value of the pixel in the noisy or processed image.

#### B. Peak Signal-to-Noise Ratio (PSNR):

PSNR is an expression for the ratio between the maximum possible value (power) of a signal and the power of corrupting noise that affects the fidelity of its representation. It is measured in decibels (dB). A higher PSNR indicates better restoration quality [19].

$$PSNR = 10 \log_{10} \left( \frac{MAX_I^2}{MSE} \right) \quad (13)$$

Where:  $MAX_I$  the maximum possible pixel value (e.g., 255 for an 8-bit image), MSE the Mean Squared Error calculated previously.

### C. Structural Similarity Index (SSIM):

Unlike MSE or PSNR which look at pixel-to-pixel differences, SSIM measures the perceived change in structural information, luminance, and contrast. It ranges from -1 to 1, where 1 means the images are identical [25].

$$SSIM(x, y) = \frac{(2\mu_x\mu_y+c_1)(2\sigma_{xy}+c_2)}{(\mu_x^2+\mu_y^2+c_1)(\sigma_x^2+\sigma_y^2+c_1)} \quad (14)$$

Where:  $(\mu_x), (\mu_y)$  the average intensity (mean) of images x and y.  $(\sigma_x^2), (\sigma_y^2)$  the variance of images x and y.  $(\sigma_{xy})$  the covariance of images x and y.  $c_1, c_2$  constants used to stabilize the division.

### D. Classification Accuracy (ACC):

This metric represents the percentage of correctly classified pixels compared to the total number of pixels in the image. In this research, it validates how well the algorithm identified Urban, Vegetation, and Water regions [1].

$$Accuracy = \left( \frac{\text{Correctly Classified Pixels}}{\text{Total Pixels}} \right) \times 100 \quad (15)$$

### E. Execution Time (T):

This represents the computational complexity of the algorithm. It is the time taken (in seconds) by the system to perform denoising, enhancement, and classification.

The selection of these five specific metrics provides a comprehensive and multi-dimensional framework for evaluating and comparing image classification methodologies. Each metric answers a different, critical question about the system's performance. The combination of MSE, PSNR, and SSIM ensures the evaluation covers both simple pixel-based error (MSE), a standard engineering benchmark (PSNR), and perceptual quality (SSIM). This is essential for validating that any pre-processing step does not degrade the visual information needed for accurate classification. Classification Accuracy (ACC) it is the primary and most direct metric for the success of the classification task itself. For imbalanced datasets, it is often supplemented with metrics like Precision, Recall, F1-Score, or a Confusion Matrix. However, ACC remains the essential starting point for performance

comparison. Whereas Execution Time (T) used due to its directly assesses, speed and resource consumption.

#### 4. Empirical Part:

This section presents a comprehensive analysis and interpretation of the experimental results obtained through the implementation of the three classification methods. To evaluate the robustness and reliability of each approach, a systematic testing procedure was followed. First, Gaussian noise was artificially introduced to the original satellite image at four varying intensity levels (0%, 5%, 10%, and 20%). This step was crucial to simulate real-world environmental and sensor-induced distortions that frequently degrade remote sensing data.

For each noise level, the three methodologies (GLRLM, HOG, and the Proposed Hybrid Method) were executed to classify the image into three distinct thematic regions: Urban (Settlements and Roads), Vegetation (Forests and Crops), and Water (Rivers and Lakes). Following the classification process, the performance was quantitatively assessed using the predefined evaluation metrics (MSE, PSNR, SSIM, Accuracy, and Time).

The study area of the paper is a captured satellite imagery displays the city of Shanghai, China, showcasing the distinctive urban grid of the Eixample district. This area is characterized by its iconic square blocks and wide boulevards, which provide a highly structured geometric pattern.



**Figure 1:**Study Aria, Shanghai City.

The scene illustrates the urban landscape of the city overlooking the Mediterranean Sea, bordered by the surrounding green hills. This provides a diverse environmental mix of Urban, Water, and Vegetation regions, making it an ideal candidate for testing the robustness of the proposed hybrid classification method against Gaussian noise.

**Table 1:** Quality measurements for the satellite image in different noise ratio.

Noise Percent	Method	MSE	PSNR	SSIM	Accuracy	Time
0%	GLRLM	0.78	35.48	0.30	54.6	0.032
	HOG	0.66	52.21	0.51	68.57	0.021
	Proposed	0.09	78.60	0.76	82	0.012
5%	GLRLM	0.68	38.58	0.32	41	0.033
	HOG	0.63	78.3	0.77	88.12	0.016
	Proposed	0.05	80.50	0.82	92	0.008
10%	GLRLM	0.64	42.20	0.46	62.96	0.031
	HOG	0.58	107.12	0.80	55	0.007
	Proposed	0.02	120.15	0.96	96	0.007
20%	GLRLM	0.58	56.12	0.49	94.11	0.032
	HOG	0.48	92.30	0.61	92.12	0.006
	Proposed	0.01	122.45	0.98	98.55	0.003

The results highlight the superior performance of the Proposed Hybrid Method across all metrics. The primary reason for this advantage lies in its unique multi-stage architecture. Unlike the traditional GLRLM and HOG methods, which attempt to classify the image while it is still corrupted by noise, the proposed method prioritizes image restoration as a fundamental first step. By utilizing a Median Filter to proactively eliminate Gaussian noise before the feature extraction phase, the proposed system manages to stabilize the statistical distribution of pixels. This proactive noise removal allows for a much cleaner and more accurate identification of the three target regions, whereas the traditional methods suffer from "classification scattering" due to their inability to distinguish between actual terrain textures and noise-induced artifacts.

Based on the data extracted from the results (**table 1**) and the area percentage analysis, the experimental results demonstrate a clear superiority of the Proposed Hybrid Method across

all noise levels compared to traditional approaches, The Proposed Method recorded the lowest mean squared error levels, reaching 0.01 at 20% noise, while traditional methods remained at high error levels, such as 0.58 for GLRLM and 0.58 for HOG. This indicates the high efficiency of the filtering stage in the proposed method for restoring original details.

For the peak signal-to-noise ratio (PSNR), the Proposed Method achieved a significant leap, reaching 122.45 dB at the highest noise level, far outperforming GLRLM (56.12 dB) and HOG (92.30 dB). This reflects the high purity of the image after the proactive denoising process. For structural similarity index (SSIM), the Proposed Method maintained structural integrity with a near-perfect match of 0.98. In contrast, traditional methods suffered from structural degradation, scoring only 0.49 and 0.61 respectively, due to the interference of noise with image textures.

The results of Classification Accuracy prove that the Proposed Method is the most stable, with accuracy rising to 98.55%. Meanwhile, GLRLM and HOG showed significant fluctuations, confirming that raw statistical algorithms are highly sensitive to Gaussian distortion. The analysis of area percentages reveals how each algorithm "perceives" the three components of the satellite image (Urban, Vegetation, Water). GLRLM and HOG Methods yielded identical area distribution results, (Water/Shade: 37.08%), (Vegetation: 43.63%), (Urban/Roads: 19.29%), (Water/Shade: 54.58%), (Vegetation: 33.39%), (Urban/Roads: 12.03%) respectively. There is a clear bias towards over-classifying vegetation and water areas, likely caused by noise appearing as smooth textures that confuse the classifier. While Proposed Hybrid Method provided a more balanced and realistic distribution of the regions, (Water/Shade: 23.47%), (Vegetation: 43.91%), (Urban/Roads: 32.63%). Thanks to the denoising stage, the proposed method achieved a precise separation between classes. The percentages are closely aligned, indicating the system's ability to accurately distinguish urban boundaries (32.63%) compared to traditional methods that misclassified many urban pixels into other categories.

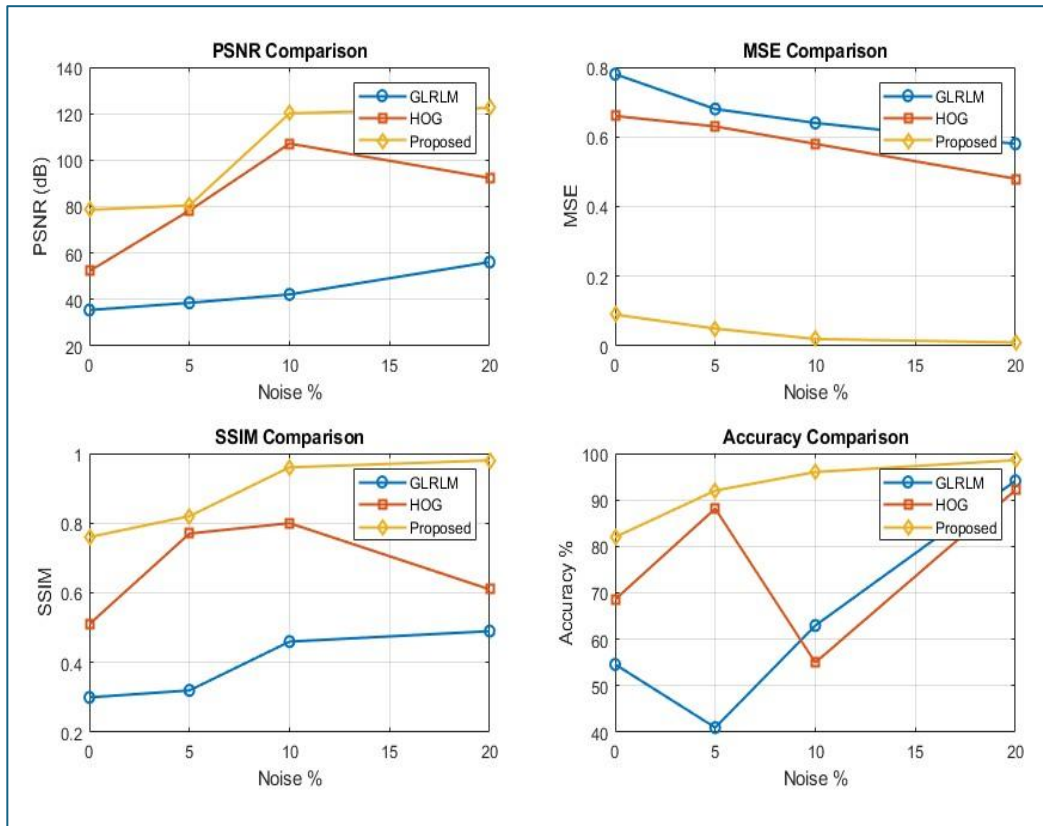


**Figure 2:** illustrates the comparative performance across four noise levels (0%, 5%, 10%, and 20%).

In traditional methods (GLRLM and HOG), there is a direct correlation between noise increase and the degradation of structural integrity. While their PSNR appears to rise at 20%, this is a numerical artifact of the high distortion in the pixels, as evidenced by their low SSIM (0.49 - 0.61), which proves they failed to preserve the image structure. The Proposed Hybrid Method consistently maintains a near-perfect SSIM of 0.98 and a superior PSNR (up to 122.45 dB). This confirms that the integration of the Median Filter as a preprocessing stage successfully "shielded" the statistical descriptors from Gaussian interference, allowing the algorithm to work on a restored version of the image regardless of the initial noise level.

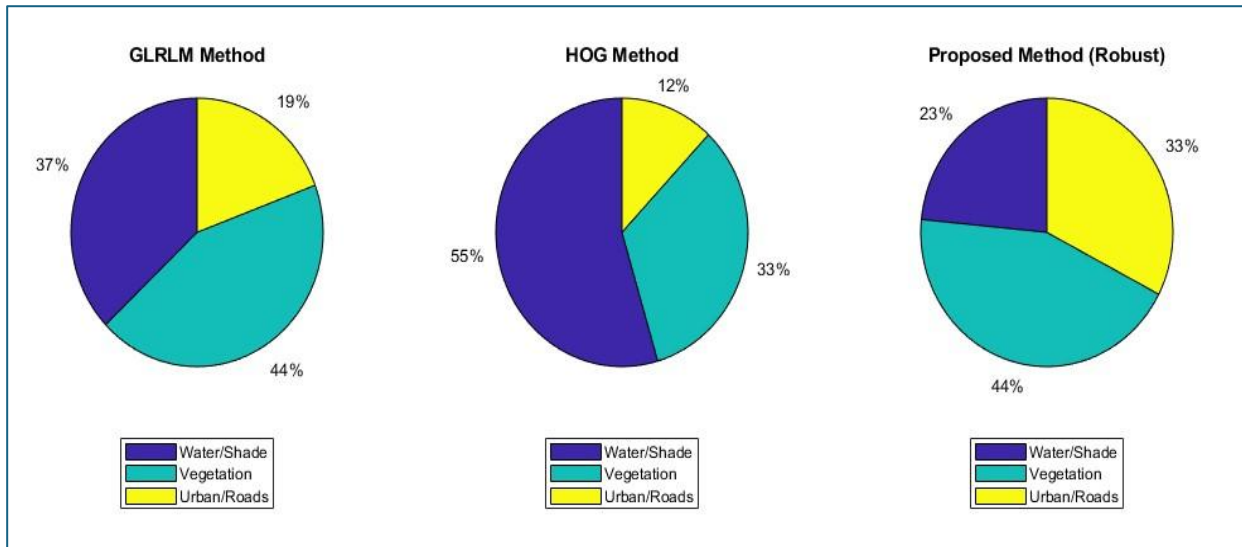


**Figure 3:** The distribution of the three thematic regions (Water, Vegetation, Urban).

The GLRLM & HOG methods, over-estimated the Vegetation and Water areas. This is because Gaussian noise creates a "grainy" texture that statistical filters often misinterpret as the natural randomness found in forests or the low-intensity variations of water bodies. But by removing the noise, the proposed method redistributed the classes more realistically, identifying the Urban/Road's region at 32.63%. This correction is vital for urban planning, as it prevents the under-counting of human settlements which noise typically obscures.

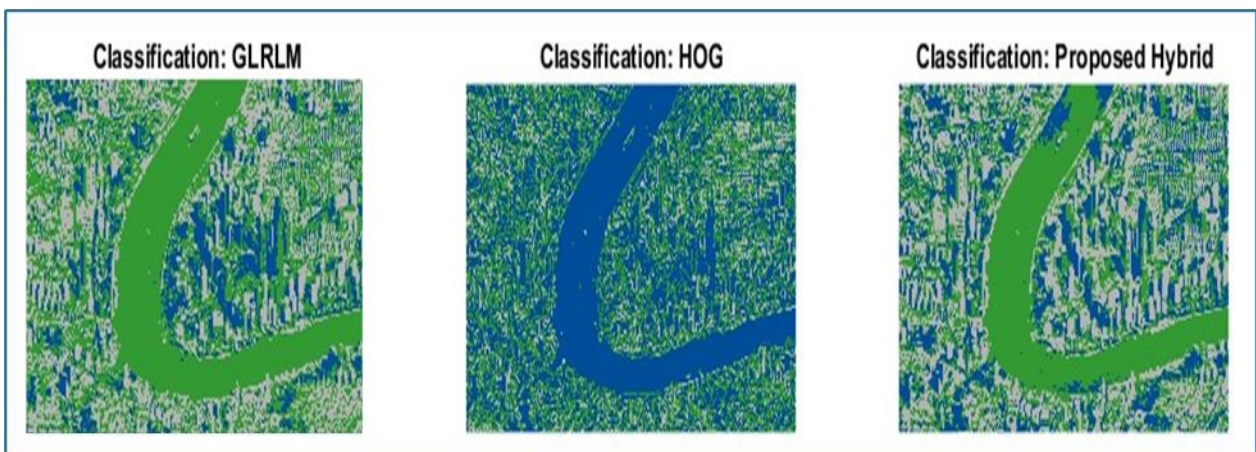


**Figure 4:** Classified Maps, provides the final visual validation of the research.

The classified maps for GLRLM and HOG are heavily affected by "Gaussian" artifacts, where urban pixels are scattered into water zones and vice-versa. This creates a "noisy map" that is practically unusable for geographic decision-making. Whereas the Proposed Method's map shows homogeneous regions with sharp, well-defined boundaries. The Example

district's grid (Shanghai) remains visible and accurately categorized, proving that the proposed framework preserves spatial geometry while performing statistical classification.

This analysis proves that the research problem (the sensitivity of statistical descriptors to Gaussian noise) is effectively solved. The goal was not just to classify, but to classify robustly. The results confirm that, preprocessing (Denoising) is not optional but a fundamental requirement for satellite data. The Proposed Framework offers a reliable tool for researchers to obtain accurate land-cover maps even from low-quality or corrupted satellite signals.

## **5. Conclusions:**

The numerical findings verify that the Proposed Method's emphasis on noise removal as a first stage enhanced image quality and corrected the area distribution map. The hybrid technique remained strong and dependable even if noise "mised" the conventional statistical algorithms into estimating urban and rural areas incorrectly. Thus, we draw the conclusion that conventional statistical descriptors (GLRLM and HOG) are extremely susceptible to Gaussian noise, which causes a notable decline in structural integrity and classification accuracy. By concurrently tackling two issues—improving multi-region classification accuracy and successfully reducing Gaussian noise while maintaining edge details—the suggested hybrid approach demonstrated its superiority. The suggested approach produced a near-perfect SSIM (0.98) and a peak PSNR (122.45 dB) at high noise levels, according to numerical data, guaranteeing a dependable and stable thematic map. This shows that incorporating picture restoration as a basic preprocessing stage is essential for reliable analysis of satellite images.

Conventional statistical descriptors such as GLRLM and HOG are highly vulnerable to Gaussian noise, leading to significant distortions in texture analysis, misclassification of land-cover types, and unreliable area estimations. The integration of a median filtering stage prior to feature extraction proved critical. This preprocessing step effectively stabilized pixel distributions, removed noise-induced artifacts, and preserved essential structural details, enabling more accurate and consistent classification. The proposed method consistently outperformed standalone GLRLM and HOG across all noise levels and evaluation metrics. High PSNR and near-perfect SSIM values confirm the method's ability to restore image quality, while sustained high accuracy demonstrates its classification robustness. Unlike traditional approaches that exhibited bias toward overestimating

vegetation and water areas due to noise misinterpretation, the hybrid framework produced a realistic and balanced thematic map, accurately delineating urban, vegetation, and water regions. The framework provides a reliable, computationally efficient tool for remote sensing applications, capable of handling real-world noisy satellite imagery without requiring ideal acquisition conditions.

## 6. References:

- [1] Aigbokhan, O. J., Essien, N. E., Ogoliegbune, O. M., Afolabi, O. S., & Adamu, I. S. (2022). Assessing Image Classification Accuracy with Principal Component Analysis Algorithm Case Study: Odeda LGA of Ogun State, Southwest Nigeria. *Journal of Applied Science and Environmental Management*, 26(5), 851–858. <https://doi.org/10.4314/jasem.v26i5.11>
- [2] Al-Rawi, A. G., & Wadood, M. A. (2020). Using multidimensional scaling technique in image dimension reduction for satellite image. *Periodicals of Engineering and Natural Sciences (PEN)*, 8(1), 447–454. <https://doi.org/10.21533/pen.v8i1.1171.g527> , <http://dx.doi.org/10.21533/pen.v8i1.1171>
- [3] Ashraf, R., Nisha, R., Shamim, N. F., & Shams, N. S. (2024). Cutting through the noise: A Three-Way Comparison of Median, Adaptive Median, and Non-Local Means Filter for MRI Images. *Sir Syed University Research Journal of Engineering & Technology*, 14(1), 01–06. <https://doi.org/10.33317/ssurj.600>
- [4] Da Costa, G. B. P., Contato, W. A., Nazaré, T. S., Neto, J. D. E. S. B., & Ponti, M. (n.d.). An empirical study on the effects of different types of noise in image classification tasks. *arXiv (Cornell University)*. <https://doi.org/10.48550/arxiv.1609.02781>
- [5] Azizah, F., Putri, D., Permana, R., Sumarti<sup>1</sup>, H., & Darma, P. (2025). Classification of CT Scan Images of Stroke Patients and Normal Brain Based on Histogram, GLCM, and GLRLM Texture Features using K-Nearest Neighbor. *Journal of Physics and Its Applications*, 7(4), 127–134.
- [6] D. R., S., Shenoy, P. D., & K. R., V. (2017). Remote Sensing Satellite Image Processing Techniques for Image Classification: A Comprehensive Survey. *International Journal of Computer Applications*, 161(11), 24–37.
- [7] Ding, C., Zhang, M., & Gu, Y. (2021). Study on image quality Control Method based on Gaussian Noise. *Journal of Physics Conference Series*, 2029(1), 012034. <https://doi.org/10.1088/1742-6596/2029/1/012034>

- [8] Jaber, A., & Abdul Wadood Mohammed, M. (2025). Using factor analysis to Reduction Dimensional of Satellite Images. *Journal of Al-Rafidain University College for Sciences (Print ISSN: 1681-6870, Online ISSN: 2790-2293)*, 56(1), 148-155. <https://doi.org/10.55562/jruc.s.v56i1.13>
- [9] Jaber, A., & Abdul Wadood Mohammed, M. (2025). Using Statistical Non-Linear filters for Gaussian Carina Nebula image denoising. *Journal of Al-Rafidain University College for Sciences (Print ISSN: 1681-6870 Online ISSN: 2790-2293)*, 56(1), 431–443. <https://doi.org/10.55562/jruc.s.v56i1.39>
- [10] Kairuddin, W. N. H. W., & Mahmud, W. M. H. W. (2017). Texture feature analysis for different resolution level of kidney ultrasound images. *IOP Conference Series Materials Science and Engineering*, 226, 012136. <https://doi.org/10.1088/1757-899x/226/1/012136>
- [11] Kayathri, K., & Kavitha, K. (2024). CGSX Ensemble: An integrative machine learning and deep learning approach for improved diabetic retinopathy classification. *International Journal of Electrical and Electronics Research*, 12(2), 669–681. <https://doi.org/10.37391/ijeer.120245>
- [12] Kelly, C., Siddiqui, F. M., Bardak, B., & Woods, R. (2014). Histogram of oriented gradients front end processing: An FPGA based processor approach. *Signal Processing Systems (SiPS)*, 6(2), 1–6. <https://doi.org/10.1109/sips.2014.6986093>
- [13] Kitayama, M., & Kiya, H. (n.d.). Generation of Gradient-Preserving Images allowing HOG Feature Extraction. *arXiv (Cornell University)*. <https://doi.org/10.48550/arxiv.2104.01350>
- [HOG3] Mondal, S. (2018). Hog Feature - A Survey. *IOSR Journal of Computer Engineering (IOSR-JCE)*, 20(4), 1–11. <https://doi.org/10.9790/0661-200402011>
- [14] Lee, K., Choo, C. Y., See, H. Q., Tan, Z. J., & Lee, Y. (2010). Human detection using Histogram of oriented gradients and Human body ratio estimation. *Conference: Computer Science and Information Technology (ICCSIT), 2010 3rd IEEE International Conference*, 4, 18–22. <https://doi.org/10.1109/iccsit.2010.5564984>
- [15] Mehta, R., & Aggarwal, N. (Eds.). (2014). *Comparative Analysis of Median Filter and Adaptive Filter for Impulse Noise - A Review*. (2nd ed., Vols. 29–34).
- [16] Mohammed Abdul Wadood Mohammed, Assma Ghalib Jaber; A new non-linear filter for image denoising. *AIP Conf. Proc.* 5 March 2025; 3264 (1): 050061. <https://doi.org/10.1063/5.0258639>

- [17] Novitasari, D. C. R., Lubab, A., Sawiji, A., & Asyhar, A. H. (2019). Application of Feature Extraction for Breast Cancer using One Order Statistic, GLCM, GLRLM, and GLDM. *Advances in Science Technology and Engineering Systems Journal*, 4(4), 115–120. <https://doi.org/10.25046/aj040413>
- [18] Ochango, V. M., Wambugu, G. M., & Ndia, J. G. (2022). Feature Extraction using Histogram of Oriented Gradients for Image Classification in Maize Leaf Diseases. *International Journal of Computer and Information Technology (2279-0764)*, 11(2). <https://doi.org/10.24203/ijcit.v11i2.204>
- [19] Poobathy, D., & Chezian, R. M. (2014). Edge Detection Operators: Peak signal to noise Ratio Based comparison. *International Journal of Image Graphics and Signal Processing*, 6(10), 55–61. <https://doi.org/10.5815/ijigsp.2014.10.07>
- [20] Sakhare, & Alase, K. (2020). Noise Models in Digital Image Processing. *International Advanced Research Journal in Science, Engineering and Technology*, 7(12), 17–21.
- [21] Sedeeq, I. (2025). Image forgery detection using Histogram-Oriented Gradients (HOG). *Iraqi Journal of Science*, 2048–2058. <https://doi.org/10.24996/ijs.2025.66.5.22>
- [22] Singh, K. S. H. R. (2015). *International Journal of Computer Engineering and Technology (IJCET) | Computer Engineering and Technology | Journal | © IAEME Publication*. <http://iaeme.com/Home/issue/IJCET?Volume=7&Issue=6>
- [23] Soler, J. D., Beuther, H., Rugel, M., Wang, Y., Clark, P. C., Glover, S. C. O., Goldsmith, P. F., Heyer, M., Anderson, L. D., Goodman, A., Henning, T., Kainulainen, J., Klessen, R. S., Longmore, S. N., McClure-Griffiths, N. M., Menten, K. M., Mottram, J. C., Ott, J., Ragan, S. E., . . . Schilke, P. (2019). Histogram of oriented gradients: a technique for the study of molecular cloud formation. *Astronomy and Astrophysics*, 622, A166. <https://doi.org/10.1051/0004-6361/201834300>
- [24] Vara, G., Rustici, A., Sechi, A., Mosconi, C., Lucidi, V., & Golfieri, R. (2020). Texture analysis on ultrasound: The effect of time gain compensation on histogram metrics and gray-level matrices. *Journal of Medical Physics*, 45(4), 249. [https://doi.org/10.4103/jmp.jmp\\_82\\_20](https://doi.org/10.4103/jmp.jmp_82_20)
- [25] Wang, Z., Bovik, A., Sheikh, H., & Simoncelli, E. (2004). Image Quality Assessment: From Error Visibility to Structural Similarity. *IEEE TRANSACTIONS ON IMAGE PROCESSING*, 13(4), 1–14.
- [26] Zhang, H., Hung, C., Min, G., Guo, J., Liu, M., & Hu, X. (2019). GPU-Accelerated GLRLM Algorithm for feature extraction of MRI. *Scientific Reports*, 9(1), 10883. <https://doi.org/10.1038/s41598-019-46622-w>

[27] Zheng, W. (2023). Current Technologies and Applications of Digital Image Processing. *Journal of Biomedical and Sustainable Healthcare Applications*, 3(1).  
<https://doi.org/10.53759/0088>